Synergy between boron nitride or graphene nanoplatelets and tri(butyl)ethylphosphonium diethylphosphate ionic liquid as lubricant additives of triisotridecyltrimellitate oil

José M. Liñeira del Río, Enriqueta R. López, Josefa Fernández*

Laboratory of Thermophysical Properties, Nafomat Group, Department of Applied Physics, Faculty of Physics, University of Santiago de Compostela, 15782, Santiago de Compostela, Spain

*Corresponding author.

E-mail address: josefa.fernandez@usc.es (J. Fernandez)

ABSTRACT: In this work, the synergy between an ionic liquid (IL) and nanoparticles as additives of lubricants was studied. For this purpose, four dispersions based on graphene nanoplatelets, GnPs, or nanoparticles of hexagonal boron nitride, h-BN, with or without the IL tri(butyl) ethylphosphonium diethylphosphate in an ester type base oil, triisotridecyltrimellitate (TTM), were prepared and tribologically analyzed as potential nanolubricants. The mass concentration of the nanoadditives is 0.1 wt%, whereas for the IL it is 2 wt%. The prepared blends were stable for three weeks. New density and viscosity values show that both properties slightly increase with the addition of IL and/or nanoparticles. Tribological tests were performed under a normal load of 20 N for TTM, the four dispersions and the TTM + 2 wt% IL mixture. With respect to base oil, a maximum friction reduction of 33% was achieved for TTM/IL/GnP nanodispersion. The best antiwear performance also corresponds to this same nanodispersion with a wear track width reduction of 44% and a strong decrease of the average cross sectional area of 65%, both respect to those obtained with the neat oil. In the case of wear scar depth, the maximum reduction is 32% for TTM/IL/h-BN nanodispersion. In addition, the values for roughness of worn surfaces tested with both TTM/IL/GnP and TTM/IL/h-BN nanodispersions are lower than those corresponding to the neat oil, to the TTM/IL mixture and to those of the corresponding binary dispersions. Hence, positive synergies between the IL and GnP or h-BN as additives of TTM were found. Confocal Raman microscopy demonstrates tribofilm formation and mending effect on worn surfaces.

KEYWORDS: ester; ionic liquid; lubricant; nanoadditives; friction: wear

1. Introduction

Recent calculations of the impact of friction and wear indicate that 23% (119 EJ) of the total energy consumption in the world takes place in tribological contacts (lubricated or not lubricated solid surfaces). 20% (103 EJ) of total consumption is used to overcome friction and 3% (16 EJ) to remanufacture worn parts and spare equipment due to wear and related faults [1]. The use of nanotechnology in the development of more efficient lubricants will reduce not only these expenses but also CO_2 emissions. In fact, the addition of a very low quantity of nanoparticles to lubricants can improve their tribological performance. Nanoparticle additives have superior tribological properties to traditional solid lubricant additives [2]. Nanolubricants are stable colloidal suspensions of nanometric materials with a very low concentration (usually lower than 1 wt%) in conventional lubricants. Hexagonal boron nitride (h-BN) based nanolubricants lead to better antifriction/antiwear capabilities compared to those of several base oils [3-7]. h-BN, considered an environmentally friendly material [8], is the softest and most lubricious polymorph of BN [9], having a lamellar crystalline structure in which van der Waals forces exist between sheets [10]. Moreover, graphene nanoplatelets (GnP) have been studied as nanoadditives [11-13] improving frictional and antiwear characteristics as well as extreme pressure properties, compared to those of some base fluids. Chang and Baek [14] have recently summarized the ecofriendly green synthesis procedures of GnP.

On the other hand, good tribological performance has been reported for ionic liquids (IL) studied as neat lubricants [15-20]. Moreover, the use of nanoadditives for ionic liquids as base oils can improve their tribological behavior [21,22]. However, ILs are still expensive and the current direction is to focus the research on the use of ionic liquids as additives [23]. In this vein, ILs based on phosphonium cations have shown a good performance as additives of biodegradable oils, among other lubricants, for steel/steel contacts [23-26].

Moreover, one of the main problems when using nanoparticles as additives is the poor stability of the resulting nanodispersions. The use of dispersants or chemical functionalization of the nanoparticles are solutions under consideration. Besides, by combining desired properties of ionic liquids and of nanoparticles, better stability and higher efficiency can be achieved [22,27,28]. Such hybrid formulations sometimes exhibit interesting positive synergies [29], but the investigations on the combined effects of ILs and uncoated nanoparticles as oil additives are still very scarce [30-33].

Senatore *et al.* [30] studied dispersions of a polyalkylene glycol base oil with both 1-ethyl-3-methylimidazolium acetate and graphene oxide (GO) as additives at two temperatures (298.15 K and 353.15 K) finding friction reductions up to 17% at 298.15 K whereas at 353.15 K no reduction was found. For the lowest GO concentration, at 298.15 K the wear reduction was 22% while for 353.15 K no reduction was obtained. On the other hand, for the highest GO concentration the wear reductions were excellent at both temperatures. Sanes *et al.* [31] found that the presence of 1-octyl-3-methylimidazolium tetrafluoroborate enhances the load-carrying and surface separating ability of graphene, leading to an unmeasurable wear, when both additives are dispersed in an isoparaffinic base oil, whereas for a SAE 10W30 fully formulated oil, no positive synergies were found for the same additives. However, tetrafluoroborate ILs are not recommended in tribology applications due to their reactivity with water leading to the production of corrosive hydrogen fluoride acid [34-36]. Amiril *et al.* [32] concluded that the addition of the IL trihexyltetradecylphosphonium bis(2,4,4-trimethylpentyl)phosphinate (1 wt%) and nanoparticles of hexagonal boron nitride (0.05 wt%) in a chemically modified palm olein trimethylolpropane ester, slightly decreases both wear (approximately 3.4%) and friction (5%) with respect to the base oil. Finally, Li *et al.* [33] investigated the synergistic effects of 2-mercaptobenzothiazolate based ILs and Mo nanoparticles in a polyethylene glycol base oil observing excellent friction-reduction and anti-wear performance at 100 °C, but not at 20 °C.

Hence, as no clear conclusion can be found, more studies on IL and nanoadditives synergies are needed.

In order to gain a deeper knowledge on the combined effects of ILs and uncoated nanoparticles as oil additives, in this work we have analyzed the synergies of tri(butyl)ethylphosphonium diethylphosphate, $[P_{4,4,4,2}][C_2C_2PO_4]$, with hexagonal boron nitride (h-BN) nanoparticles and with graphene nanoplatelets (GnPs) using triisotridecyltrimellitate (TTM) as base oil. There is no previous research on the tribological synergies of both graphene nanoplatelets and ILs as additives of base oils. Recently, Oulego *et al.* [37] have determined the bacterial toxicity of seven phosphonium ILs previously analyzed as lubricant additives. These authors conclude that the IL tri(butyl)ethylphosphonium diethylphosphate, $[P_{4,4,4,2}][C_2C_2PO_4]$, was the least toxic of all the ILs tested. The main advantages of trimellitate esters are low volatility, good thermal stability, good stability to oxidation, high film strength, good low temperature properties, high flashpoints and good hydrolytic stability. Trimellitate esters are used as specialty lubricants including compressor fluids, two stroke oils, greases or chain oils [38].

2. Experimental section

2.1. Materials

The triisotridecyltrimellitate sample (TTM, CAS Number: 72361-35-4, Fig. 1) was provided by Verkol. This oil has been characterized by infrared spectroscopy (IR) with a FTIR Varian 670-IR spectrometer. The spectrum (Fig. 2) shows the following peaks: a strong peak at 1726 cm^{-1}, which corresponds to the stretching vibration of ester carbonyl (C=O), two weak peaks around 1574 and 1607 cm^{-1} that are associated with the C-H stretching in-of plane ring, some peaks appear around 1305–1240 cm^{-1} related to C–O(H) stretching and C–O–(H) bending vibrations, a peak at 1102 cm^{-1}, which can be assigned to the (C–O–C) single bond stretching

vibration and some peaks at 2956 cm^{-1}, 2927 cm^{-1} and 2871 cm^{-1} which correspond to carbon–hydrogen groups: (CH_3) asymmetric stretching, (CH_2) asymmetric stretching and (CH_3) symmetric stretching respectively [39,40].

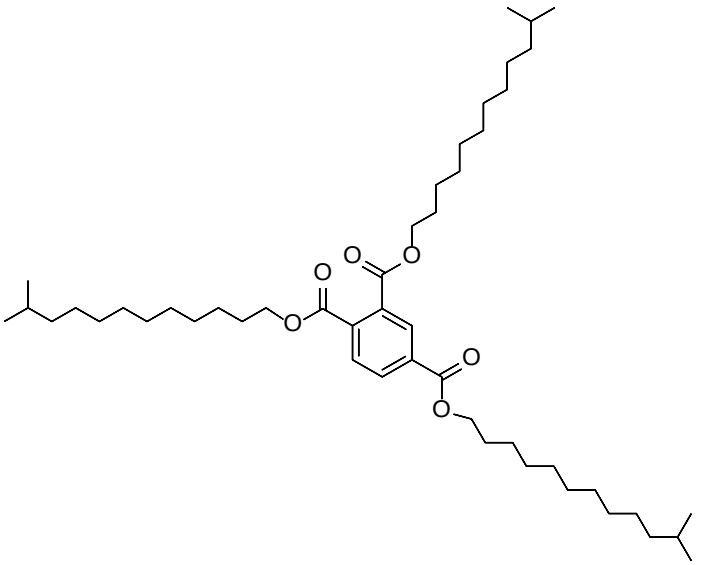

Fig. 1. Chemical structure of triisotridecyltrimellitate (TTM).

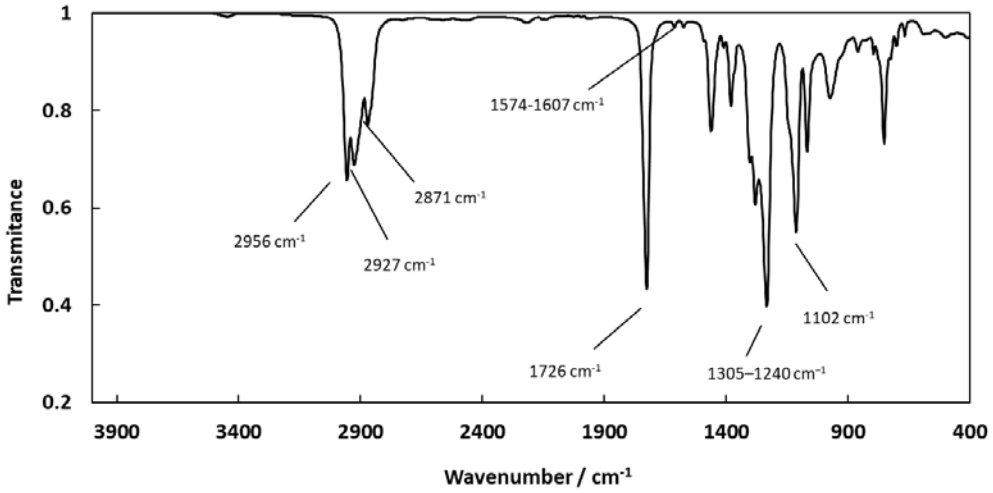

Fig. 2. The FTIR spectrum of triisotridecyltrimellitate (TTM) base oil.

Moreover, this base oil was also analyzed by high performance liquid chromatography, HPLC, coupled with a quadrupole orthogonal acceleration time-of-flight mass spectrometer (microTOF-Q™) which is equipped with an electrospray ionization source (ESI). The base oil was dissolved in isopropanol (5:250) and analyzed in isocratic mode. As can be seen in Fig. 3,

a wide peak appears, which may be due to small impurities similar to triisotridecyltrimellitate. The mass spectrum (Fig. 4) of the oil, shows that the mass of the molecular ion corresponds to TTM (molecular weight 757.63 g·mol^{-1} and molecular formula: $C_{48}H_{84}O_6$). Moreover, this spectrum shows another weak peak with a molecular weight close to that of TTM; this fact may be owing to the loss of some hydrogen atoms in the molecule. To the best of our knowledge no previous mass spectra of this type of esters have been reported. The TTM kinematic viscosity at 40ºC and its viscosity index are 317 cSt and 74, respectively [24].

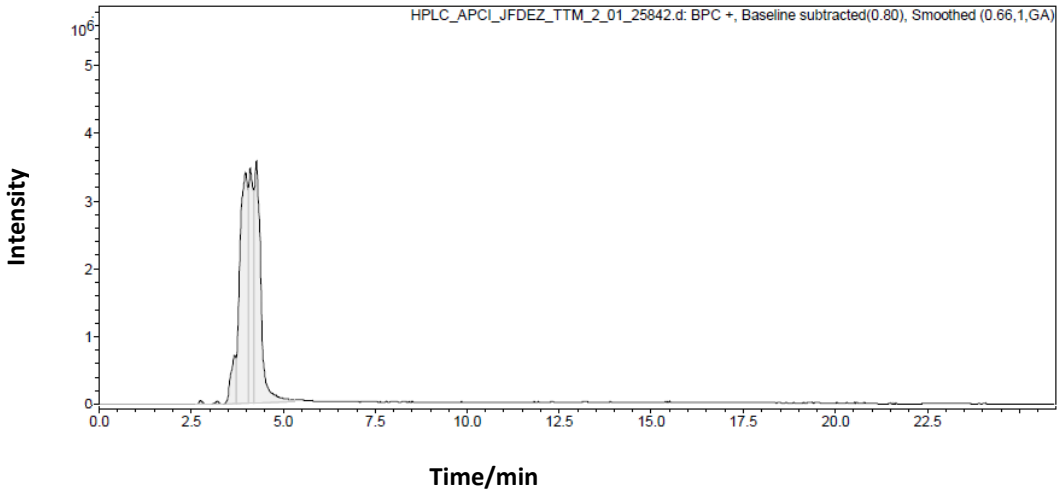

Fig. 3. HPLC chromatogram of the triisotridecyltrimellitate sample.

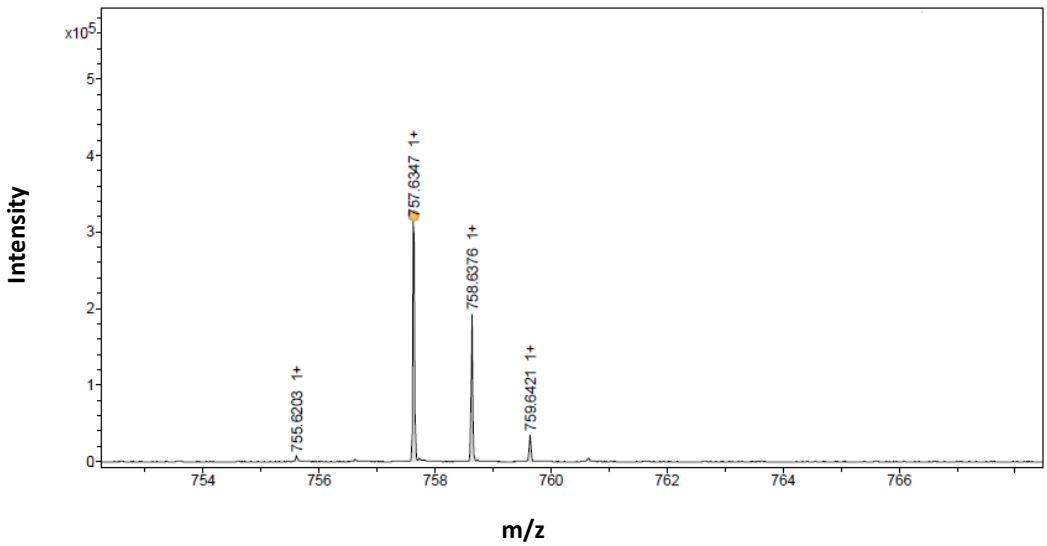

Fig. 4. Mass spectrum of TTM (retention time 4.0 min).

Hexagonal boron nitride powders (h-BN, CAS Number: 10043-11-5) have a purity of 99.5 %, an average particle size of 70 nm and a specific average area of 19.4 m^2/g as indicated

by the manufacturer (Iolitec, GmbH, Germany, lot MNC018001). An aliquot of the powder sample has previously been characterized [41]. Disc-like shaped morphology was obtained for h-BN nanoparticles with Transmission Electron Microscopy (TEM) [41]. Graphene nanoplatelets powders (GnP, CAS number 1034343-98-0) of a purity of 99.5% with an average particle diameter of 15 μm and a thickness of 11-15 nm, were also provided by Iolitec. An aliquot of this GnP sample was used in a previous work [11] where its properties are described. Tri(butyl)ethylphosphonium diethylphosphate ($[P_{4,4,4,2}][C_2C_2PO_4]$, Cyphos® 169, CAS Number: 20445-94-7, Fig. 5) was kindly provided by Cytec Industries Inc. (US) with a purity of 96.3%. Its kinematic viscosity at 40ºC and the viscosity index are 225 cSt and 82 [24], respectively. FTIR and Raman spectra of this IL are shown in Figs. S1 and S2 respectively. A band with three peaks at 2873, 2927 and 2958 cm^{-1} due to the methylene bonds of the aliphatic chains can be observed in Fig. S1. FTIR spectrum also shows a single peak at 1148 cm^{-1} that can be assigned to the P=O bond. The full spectrum is very similar to that previously reported for the same IL by Hernández Battez *et al*. [42]. A WITec alpha300R+ confocal Raman microscopy was used to obtain the Raman spectrum of the IL. We are not aware of any previous Raman spectrum of this IL reported in the literature.

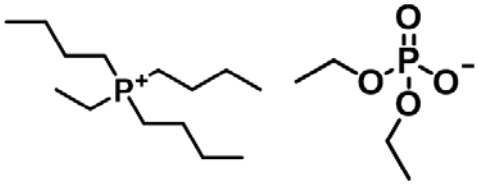

Fig. 5. Chemical structure of tri(butyl)ethylphosphonium diethylphosphate, $[P_{4,4,4,2}][C_2C_2PO_4]$.

2.2. Preparation of the nanolubricants

Four dispersions were prepared apart from a mixture of TTM and $[P_{4,4,4,2}][C_2C_2PO_4]$ with a concentration of 2 wt% of the IL. Two-step method was used to make the nanodispersions TTM + 0.1 wt% h-BN and TTM + 0.1 wt% GnP. To prepare TTM + 2 wt%

157 IL + 0.1 wt% h-BN and TTM + 2 wt% IL + 0.1 wt% GnPs nanodispersions, a procedure similar
158 to that used by Sanes *et al.* [31] was employed. Firstly, h-BN or GnP nanopowders were added
159 to the IL. Secondly, this ensemble is mechanically mixed in an agate mortar for 5 min and
160 subsequently mixed with the base oil (TTM). The four nanodispersions were sonicated for 4
161 hours by ultrasound in a Fisherbrand bath, operating in continuous shaking mode with an
162 effective power of 180 W and a sonication frequency of 37 kHz. The weight percentage of all
163 the blends was determined by using a Sartorius balance (model MC 210P) with a readability of
164 0.01 mg. The mass concentration of the nanoparticles was chosen due to good tribological
165 performance obtained in our previous research [11,43]. Stability of the nanodispersions were
166 analyzed by visual observation and the measurement of the refractive index along time by using
167 a Mettler Toledo Refractometer RA-510M. Its measuring cell is an inverted cone-shaped cavity,
168 with stainless steel walls. The base of this cone is a polished surface of a sapphire prism, on
169 which the nanolubricant is placed. In addition, in order to analyze the interactions among the
170 components of the nanodispersion the FTIR Varian 670-IR spectrometer was used.

171 *2.3. Thermophysical Measurements*

172 Density and dynamic viscosity of the lubricants were measured from 278.15 to 373.15
173 K and at atmospheric pressure with a rotational Stabinger viscometer SVM 3000 from Anton
174 Paar (Graz, Austria) which incorporates a vibrating tube densimeter [44]. This device has
175 previously been described in detail [45,46]. The expanded uncertainties (k = 2) are 1% for
176 dynamic viscosity, 0.0005 $g \cdot cm^{-3}$ for density and 0.02 K for the temperature from 288.15 to
177 378.15 K and 0.05 K outside this range.

178 *2.4. Tribological Tests*

179 Rotational friction tests were performed with a CSM Standard tribometer working in a
180 ball-on-disc configuration [43] for the base oil, the TTM + IL mixture and the four
181 nanodispersions at room temperature (~23ºC) under the following conditions: load of 20 N

(maximum contact pressure of 1.8 GPa), trajectory radius of 3 mm, sliding distance of 340 m and speed of 0.10 $m \cdot s^{-1}$. The specimens used were chrome steel balls (AISI 52100/535A99; 6 mm of diameter; hardness: 58–66 Rockwell Scale; roughness < 0.05 μm) and stainless-steel discs (AISI 52100/535A99; 10 mm diameter; surface finish < 0.02 μm Ra; hardness: 190-210 Hv30). Before each test, both disc and ball were cleaned in an acetone ultrasonic bath in order to eliminate any type of substance that could interfere in our studies and dried under hot air. Subsequently, the disc was lubricated with four drops of the lubricant under study. At least three replicates were performed.

Once the friction tests were done, in order to analyze the wear, the discs were washed in an ultrasonic bath with acetone. The wear that appears on the discs after the tribological tests was characterized with a 3D Optical Profiler Sensofar S Neox (confocal mode, 10x) in terms of wear track width (WTW), wear track depth (WTD) and cross-section area. With the aim of obtaining representative average values, the width, depth and cross-section area of the wear scar were measured in three different zones. A Carl Zeiss FESEM ULTRA Plus Scanning Electron Microscope (SEM) was used to analyze the morphology of the worn surface. Furthermore, the WITec alpha300R+ confocal Raman microscopy was used to obtain information about the composition in the wear track.

3. Results and discussion

3.1. Stability of the dispersions

Stability of the prepared nanolubricants was estimated by visual observation, which consists in observing how the nanoparticles deposit over time. As can be seen in Fig. 6, no signs of sedimentation appeared for the first three weeks after the nanolubricant preparation. This time is longer than that needed to perform the tribological assays, which is about 5 hours for each dispersion.

Moreover, in order to analyze the stability of nanoparticles against sedimentation in the base oil, the refractometry technique was used [43,47,48]. For this task, the refractive index of each nanolubricant was measured every hour until 100 hours, observing its evolution over time (Fig. 7). The refractive index is determined when the refracted ray is parallel to the polished surface where the nanoparticles sediment. As the number of sediment nanoparticles grows, the refractive index increases. In a previous research [43] we analyzed the refractive index of graphene oxide (GO) and reduced graphene oxide (rGO) nanolubricants based on two different base oils. Results of this work show that after 100 hours for both base oils the refractive index grew over 0.4% and 0.1% for GO and rGO nanolubricants, respectively. Guimarey *et al*. [48] studied the stability of ZrO_2 nanoparticles in different base oils also through refractive index evolution. In this last work, the refractive index showed an increase of around 0.4% for two base oils after 100 hours of study. In the present work, the refractive index evolution over 100 hours shows an increase of around 0.1 and 0.2 % for nanolubricants with and without IL, respectively, indicating a good stability of nanoparticles and also that the presence of IL improves stability.

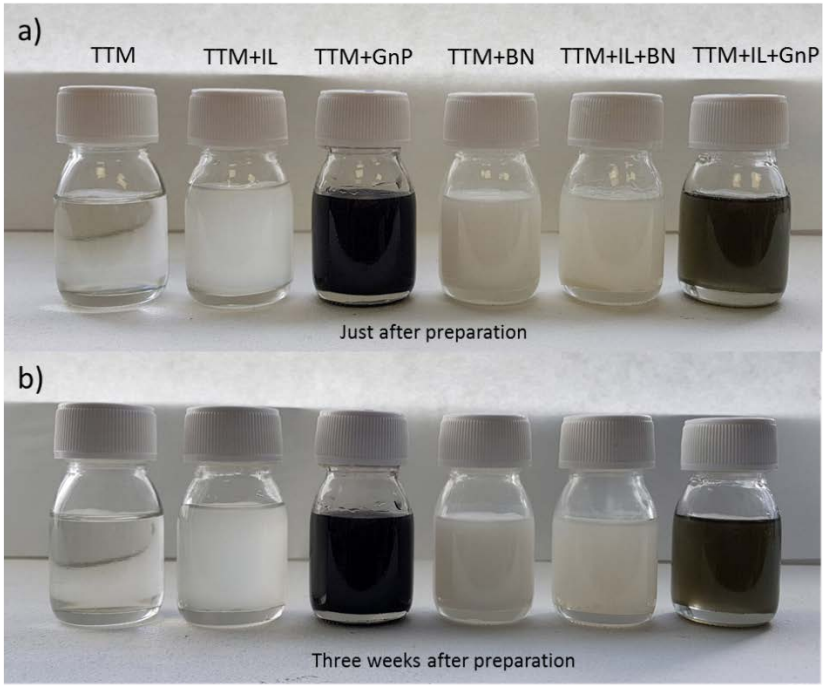

Fig. 6. Visual observation of nanolubricants stability a) just after sonication b) three weeks after sonication.

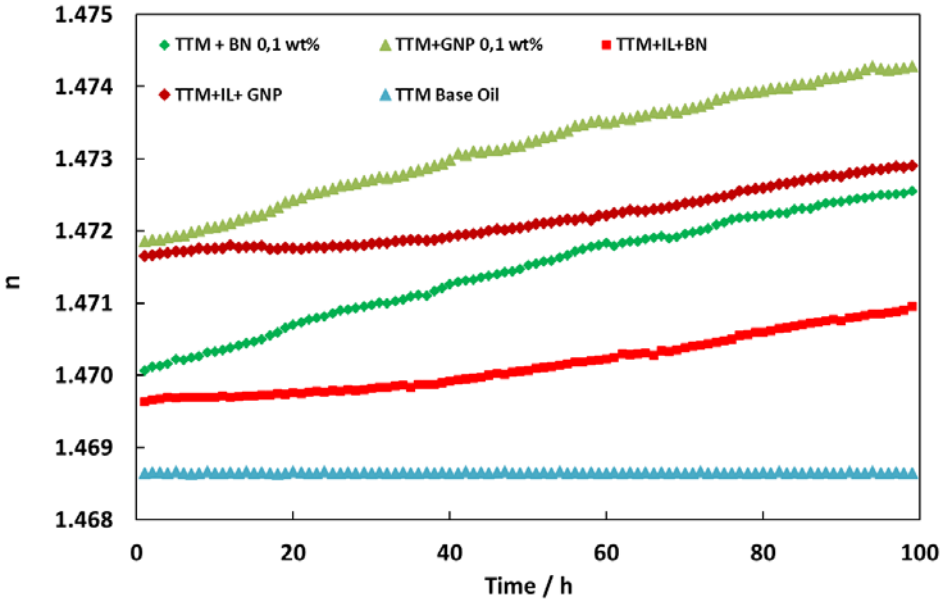

Fig. 7. Temporal evolution of the refractive index, n, for the different prepared nanolubricants and TTM base oil.

The comparisons among the FTIR spectrum of the base oil with those for the different lubricants additivated with IL and/or nanoparticles are presented in Fig. 8. In these spectra it is clearly shown that no new peaks appear for nanolubricants in comparison with the base oil without additives. Therefore, it can be concluded that for the used nanolubricants no chemical bonds are formed between base oil and additives. Nevertheless, it should be taken into account that at this low concentration of additives if new chemical bonds are formed, they might not be observed.

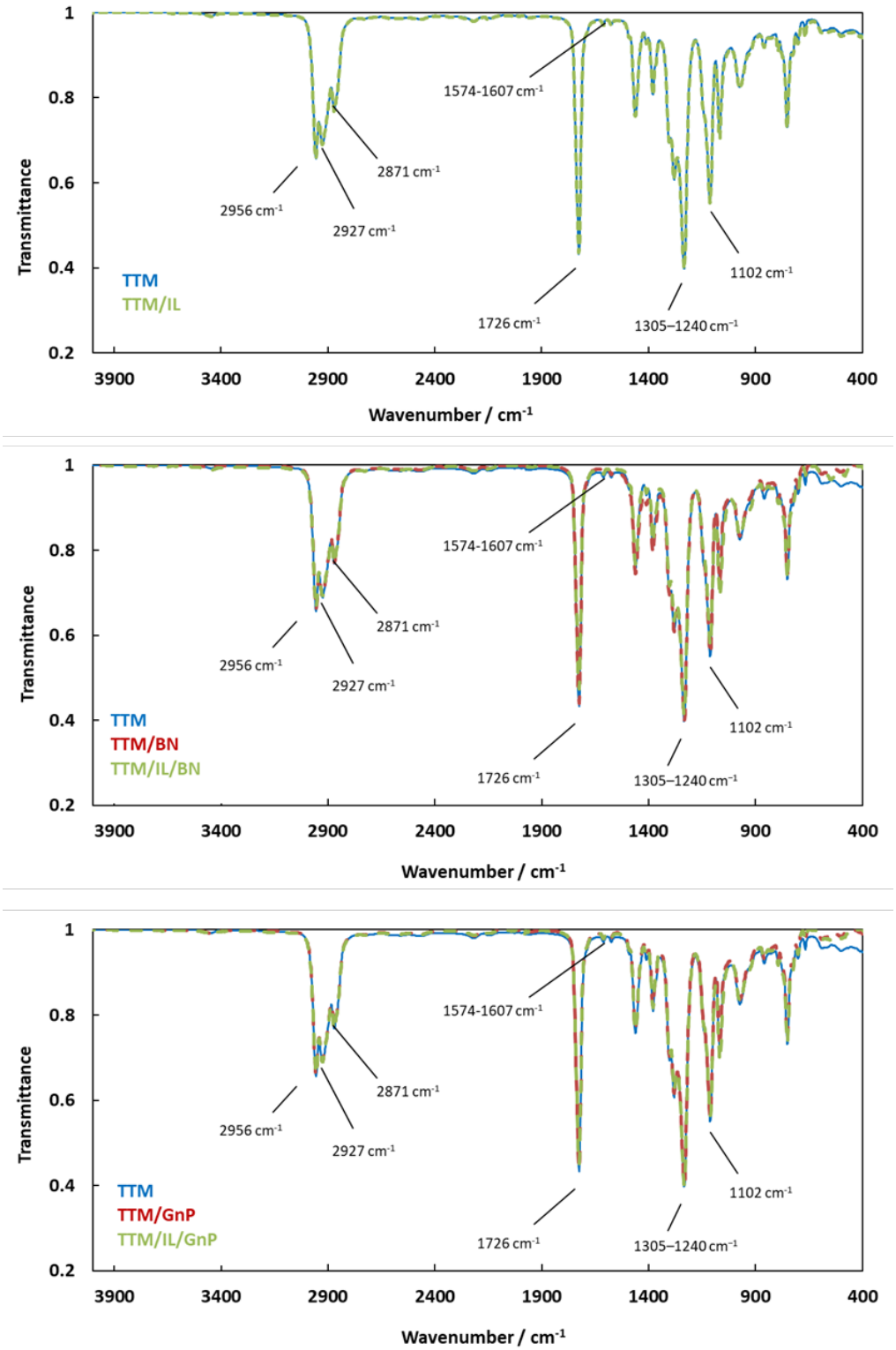

Fig. 8. FTIR spectra of the studied lubricants.

3.2. Thermophysical Properties

Densities and viscosities for the nanolubricants and base oil are presented in Tables 1 and 2 respectively. For the entire temperature range, both properties, density and viscosity, slightly rise with the addition of additives (IL and nanoparticles) in comparison to base oil. The highest density and viscosity values were obtained with the TTM/IL/GnP nanolubricant. Specifically, the maximum increase in density with respect to TTM is 0.23% at 368.15 K whereas in the case of viscosity the maximum increase is 9.6 % at 338.15 K. The largest increase in viscosity of TTM due to the IL is 7.9% at 338.15 K.

Table 1. Experimental density, ρ / g·cm^{-3}, of the nanodispersions, IL mixture and base oil as a function of temperature.

T/K	ρ / g cm^{-3}					
	TTM	*TTM + h-BN*	*TTM + GnP*	*TTM + IL*	*TTM + IL+ h-BN*	*TTM + IL+ GnP*
278.15	0.9648	0.9652	0.9649	0.9658	0.9657	0.9663
283.15	0.9616	0.9619	0.9616	0.9625	0.9623	0.9630
288.15	0.9581	0.9586	0.9583	0.9592	0.959	0.9597
293.15	0.9550	0.9552	0.9550	0.9559	0.9557	0.9563
298.15	0.9514	0.9519	0.9516	0.9526	0.9524	0.9530
303.15	0.9481	0.9485	0.9483	0.9493	0.9490	0.9497
308.15	0.9442	0.9451	0.9449	0.9459	0.9456	0.9463
313.15	0.9412	0.9418	0.9415	0.9426	0.9423	0.9429
318.15	0.9380	0.9385	0.9382	0.9393	0.9389	0.9396
323.15	0.9344	0.9352	0.9348	0.9360	0.9356	0.9363
328.15	0.9312	0.9319	0.9315	0.9327	0.9323	0.9330
333.15	0.9278	0.9286	0.9282	0.9294	0.9290	0.9297
338.15	0.9250	0.9252	0.9249	0.9261	0.9257	0.9263
343.15	0.9213	0.9219	0.9215	0.9227	0.9223	0.9230
348.15	0.9178	0.9186	0.9182	0.9194	0.9190	0.9197
353.15	0.9146	0.9152	0.9149	0.9161	0.9156	0.9163
358.15	0.9110	0.9119	0.9115	0.9127	0.9123	0.9130
363.15	0.9081	0.9086	0.9082	0.9094	0.9089	0.9097
368.15	0.9042	0.9052	0.9049	0.9060	0.9056	0.9063
373.15	0.9011	0.9019	0.9015	0.9027	0.9023	0.9030

Table 2. Experimental dynamic viscosity, η / mPa·s, of the nanodispersions, IL mixture and base oil as a function of temperature.

T/K	η / mPa·s					
	TTM	*TTM + h-BN*	*TTM + GnP*	*TTM + IL*	*TTM + IL+ h-BN*	*TTM + IL+ GnP*
278.15	6806	6855	6820	6936	6903	6980
283.15	3916	3943	3931	3993	3986	4033
288.15	2360	2377	2372	2407	2409	2454
293.15	1472	1485	1482	1505	1508	1538
298.15	954.4	958.8	955.7	971.9	974.1	984.3
303.15	621.6	637.6	636.0	646.6	648.6	661.0
308.15	429.3	436.4	435.6	442.4	443.9	452.6
313.15	302.3	306.5	306.1	310.4	311.8	316.5
318.15	216.0	220.6	220.2	223.3	224.2	225.9
323.15	158.8	162.3	162.1	164.2	164.8	166.2
328.15	116.0	122.0	121.8	123.3	123.7	125.7
333.15	89.97	93.37	93.38	94.33	94.60	95.82
338.15	68.01	72.80	72.90	73.40	73.53	74.53
343.15	55.01	57.69	57.84	58.03	58.09	58.94
348.15	44.97	46.40	46.60	46.52	46.47	47.25
353.15	35.16	37.84	38.08	37.81	37.76	38.46
358.15	29.87	31.25	31.52	31.13	31.07	31.61
363.15	25.11	26.11	26.39	25.94	25.89	26.48
368.15	21.02	22.05	22.33	21.86	21.83	22.29
373.15	17.68	18.81	18.06	18.57	18.53	18.91

3.3. Tribological Characterization

In Fig. 9 the mean values of the coefficients of friction (μ) for all studied lubricants based on TTM has been plotted. The friction coefficients obtained lubricating the contact with each of the four nanodispersions and the IL mixture are lower than the one corresponding to using TTM without additives. The highest friction reduction was obtained for the nanolubricant TTM + 2 wt% IL + 0.1 wt% GnPs. For this last nanolubricant, a friction coefficient of 0.0836 was obtained against 0.125 for the base oil (Table 3). Thus, the obtained friction reductions with respect to base oil range from 14% (for the TTM/IL mixture) to 33% (for the TTM/IL/GnP nanodispersion), being the relative reduction in the friction coefficient: $100\left(\left(\mu_{oil} - \mu_{dispersion}\right)/\mu_{oil}\right)$.

Table 3. Mean values of the friction coefficient, μ, and of the width, WTW, depth, WTD, and cross-section area of the wear track and their respective standard deviations for all lubricants.

Dispersion	μ	σ	WTW/μm	σ/μm	WTD/μm	σ/μm	Area/μm^2	σ/μm^2
TTM	0.1253	0.0043	344	22	1.29	0.42	274	17
TTM+ 0.1 wt% h-BN	0.1076	0.0035	246	20	0.95	0.25	120	18
TTM+0.1 wt% GnP	0.1036	0.0060	242	21	1.23	0.19	142	12
TTM+ 2 wt% IL	0.1077	0.0096	234	18	1.21	0.37	140	14
TTM+2 wt% IL+ 0.1 wt% h-BN	0.1019	0.0043	223	19	0.88	0.51	120	12
TTM+2 wt% IL+ 0.1 wt% GnP	0.0836	0.0048	194	16	1.19	0.34	110	16

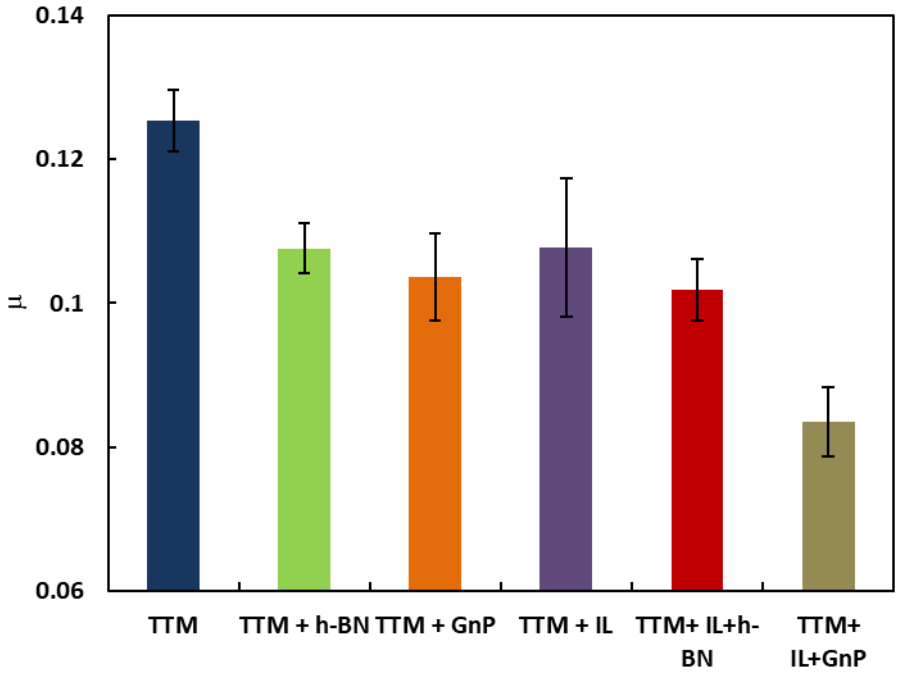

Fig. 9. Mean friction coefficient, μ, obtained for all the studied lubricants.

As can be seen in Table 3, the wear obtained with all the prepared dispersions is lower than for the base oil without additives. The mean wear track width reduction ranges from 28% (for the TTM/h-BN nanodispersion) to 44% (for the TTM/IL/GnP nanodispersion), the improvements in the mean wear track depth range from 5% (for the TTM/GnP nanodispersion) to 32% (for TTM/IL/h-BN nanodispersion) whereas the decrease of the average cross sectional area (Fig. 10) is excellent for all the cases ranging from 56% (for the TTM/GnP mixture) to 66% (for TTM/IL/GnP nanodispersion). Consequently, the nanodispersions containing ILs provide better tribological properties than the TTM/IL mixture and the corresponding

nanodispersion without IL. On the other hand, the friction and wear reductions of the TTM/IL/h-BN nanodispersion (19% and 32% respectively) are significantly better than those obtained by Amiril *et al.* [32] for an ester/IL/h-BN lubricant (5% and 3.4%) and those obtained by Senatore *et al.* [30] at 298. 15 K for a glycol/IL/GO nanodispersion (17% and 22%).

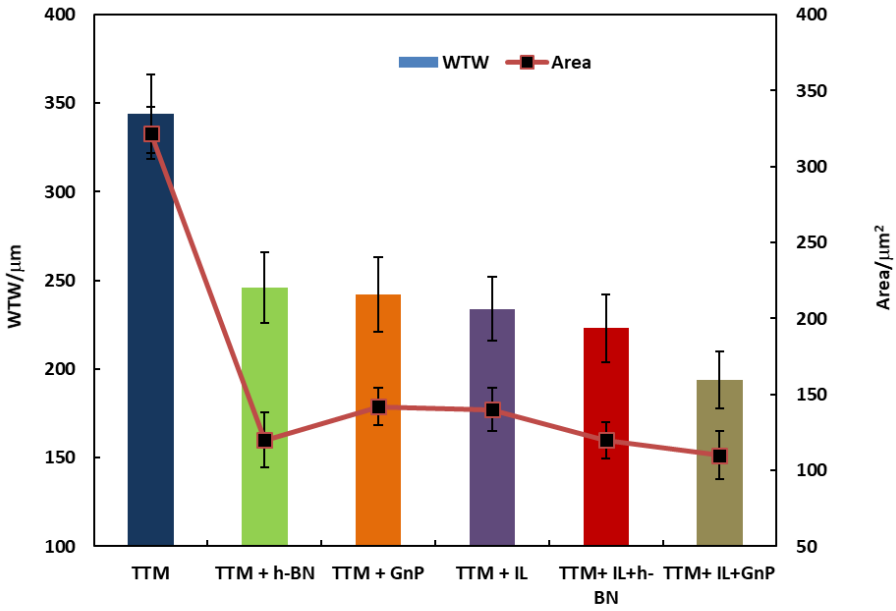

Fig. 10. WTW and transversal area obtained for all the studied lubricants.

In Fig. 11 a significant reduction can be observed in the 3D profiles of the wear tracks obtained lubricating the contact with the TTM/IL/GnP nanodispersion in comparison with that corresponding to neat oil. Profiles of the transversal areas and 3D profiles of worn surfaces for all the studied lubricants are shown in Fig. 12, where the reductions of the scars are clearly observed, especially for the TTM + 2 wt% IL + 0.1 wt% GnP nanodispersion.

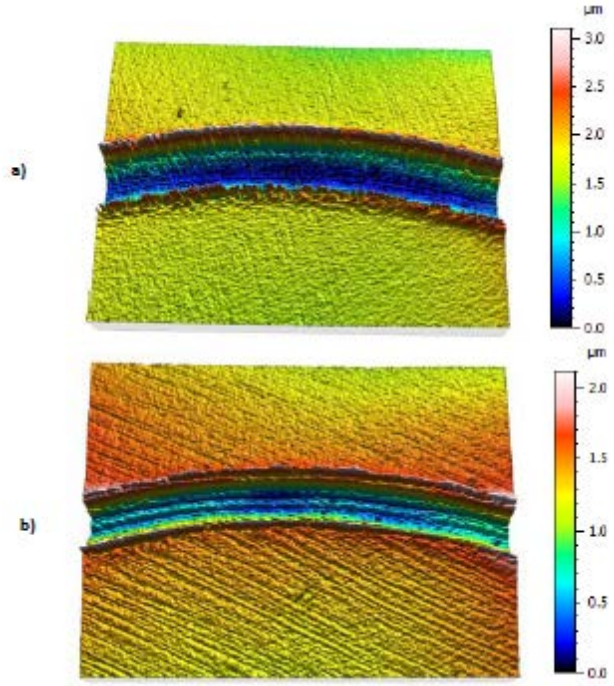

Fig. 11. 3D profiles (Confocal 10x) of the wear tracks of the discs lubricated with (a) TTM base oil (b) nanolubricant formed by TTM + 2 wt% IL + 0.1 wt% GnP

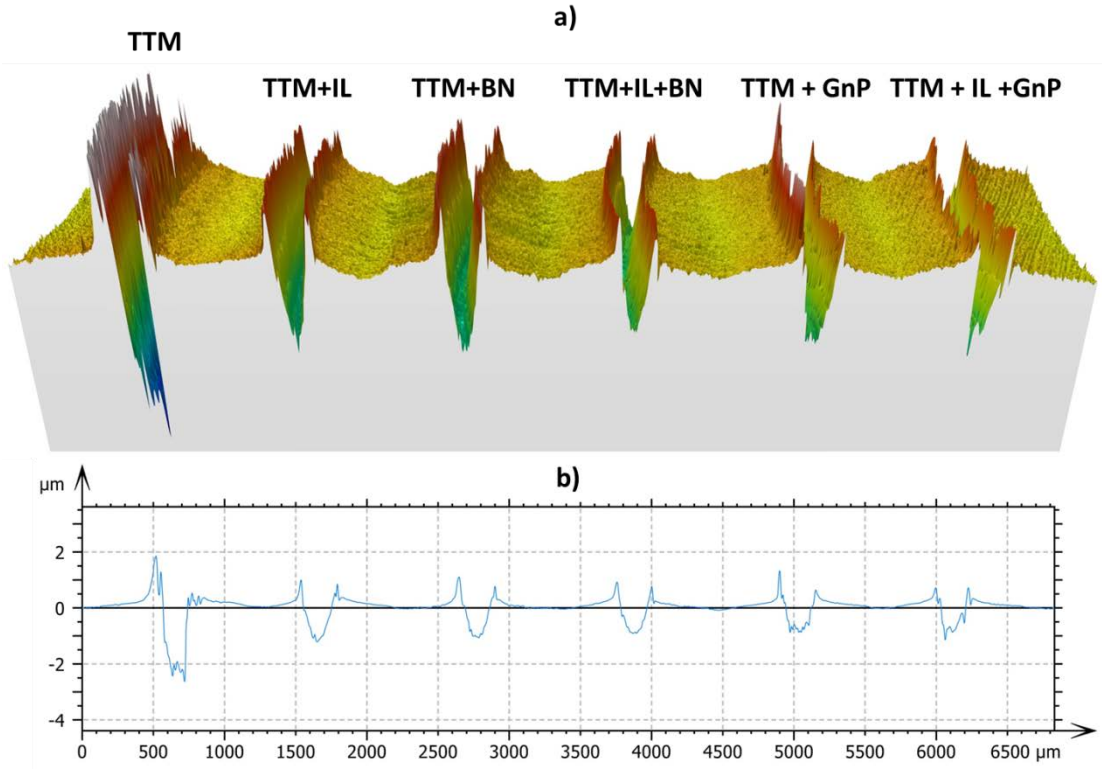

Fig. 12. a) 3D Surface topography of wear tracks and b) Cross section profiles of wear tracks for the all the studied lubricants at room temperature.

Different mechanisms have been identified to explain the role of nanoparticles as lubricant additives. These mechanisms are classified in two different categories: direct effect

of the nanoparticle on the surface (ball bearing and tribofilm formation) and surface enhancement effects (mending and polishing effects) [49,50]. As regards the role of ionic liquid, the main mechanism is the formation of tribofilm. In order to better understand the mechanisms underlying in the present samples, we have performed measurements of roughness, SEM and Raman microscopy.

The roughness of the worn surface, *Ra*, was determined according to the standard ISO 4287, applying a Gaussian filter with a long wavelength cut-off of 0.25 mm. As presented in Table 4, the roughness values of the worn surface, *Ra*, corresponding to TTM+IL, TTM+h-BN and TTM+GnP are 8.8, 8.3 and 7.9 nm respectively. Taking into account that the roughness value of the worn surface of TTM base oil was 19.7 nm, we can conclude that the presence of the chosen IL produces the formation of protective tribofilms whereas the nanoadditives can lead to mending, polishing or tribofilm formation effects. The smoothest surface corresponds to the disc lubricated with the TTM/IL/GnP nanodispersion (*Ra* = 7.0 nm) followed by the one lubricated with the mixture TTM/IL/h-BN (*Ra* =7.5 nm). Thus, positive synergies between the IL and the both nanoadditives were found.

Table 4. Roughness parameter, *Ra*, of worn surfaces for the different analyzed nanolubricants.

Lubricant	*Ra* / nm	σ / nm	Gaussian Filter / mm
TTM base oil	19.7	1.2	0.25
TTM +h-BN	8.29	0.64	0.25
TTM + GnP	7.91	0.55	0.25
TTM +IL	8.82	0.52	0.25
TTM +IL+ h-BN	7.47	0.51	0.25
TTM +IL+ GnP	7.02	0.46	0.25

Moreover, SEM micrographs of wear tracks after lubrication with all the studied lubricants based on TTM were performed. Fig. 13 (especially Fig. 13b) shows abrasive wear scratches for the scar corresponding to the neat oil whereas for the scars corresponding to the five additivated TTM oils, plastic deformation and smoother surfaces were found in agreement with roughness values. Additionally, for the nanolubricant TTM/IL/GnP an important decrease

in wear scar width is observed in comparison with the base oil TTM as seen in Fig. 13a. These results confirm the wear measurements analyzed with the 3D profilometer.

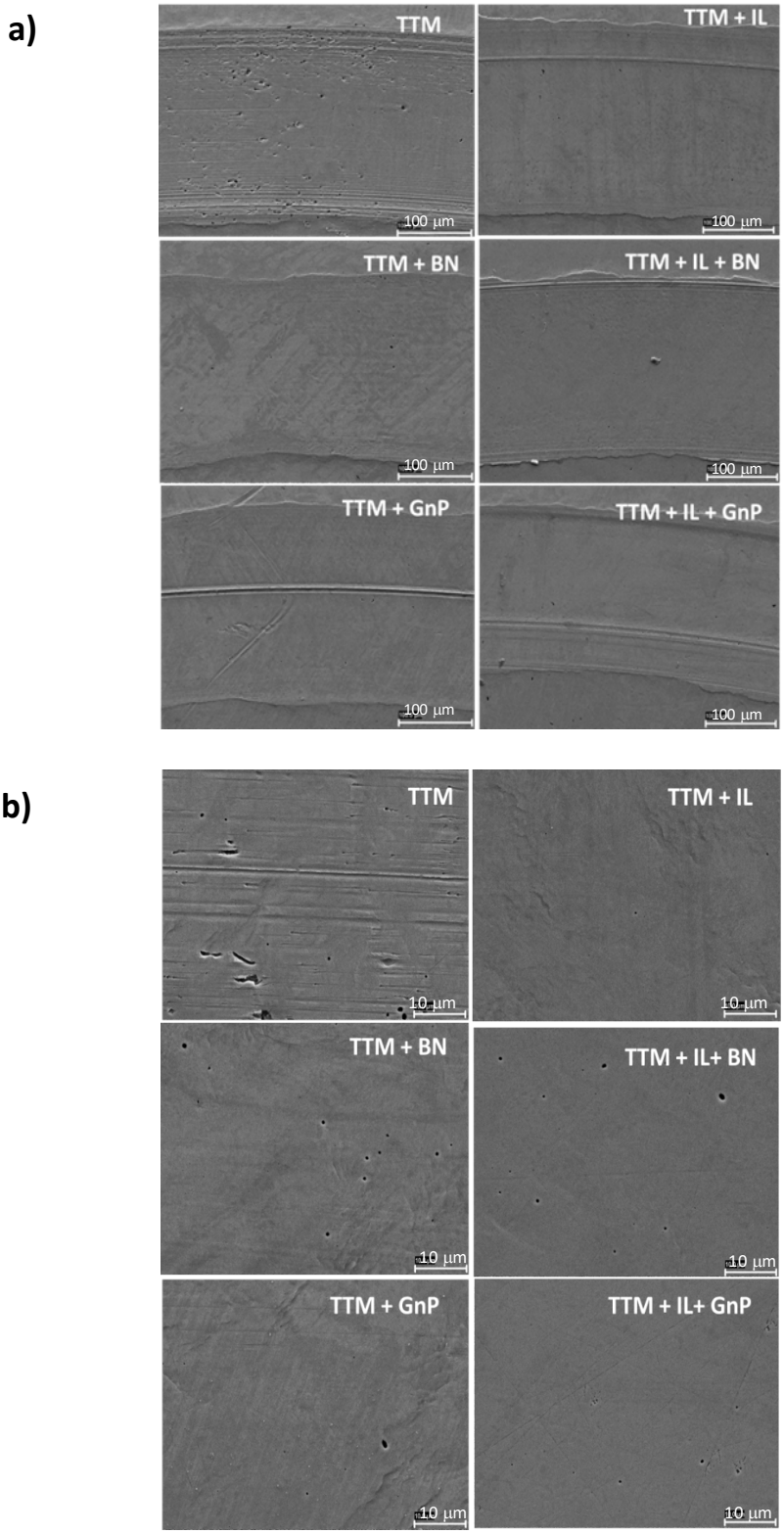

Fig. 13. SEM micrographs a) 700x and b) 5000x for the worn discs after tribological tests for the studied nanolubricants.

Elemental mapping and Raman spectra of the three additives (Figs. S2-S4) and of the worn surfaces lubricated with TTM and with the five additivated TTM oils (Figs. S5-S8 and 14) were recorded with a confocal Raman microscope at a wavelength of 532 nm in order to know the role that nanoparticles and the ionic liquid play in the reduction of surface wear of discs. An important tribofilm is evidenced due to a significant presence of IL (blue color) in the mapping of the worn surface lubricated with the TTM/IL mixture. (Fig. S6). On the other hand, the Raman spectrum of the h-BN powders (Fig S4) exhibits a characteristic band at 1367 cm^{-1} [51] that is due to the E2g phonon mode, similar to the G band in graphene or graphene derivatives [11]. The spots of boron nitride nanoparticles (Fig. S7) on the worn surface lubricated with TTM/h-BN dispersion, as well as roughness reduction could indicate the occurrence of mending effect.

The spectrum of the GnP nanopowders (Fig. S3) shows two characteristic bands around 1350 cm^{-1} (D-band) and at 1580 cm^{-1} (G-band) [11]. The first one is a result of the breathing modes of sp^2 atoms in rings whereas the G-band is due to the bond stretching of all pairs of sp^2 atoms in rings and chains [11,52]. On the worn surface lubricated with TTM/GnP dispersion (Fig. S8) the presence of areas where the spectrum coincides with that of GnP can be observed (Fig S3). Taking this last result into account, as well as the roughness and SEM images it can be concluded that there is a presence of mending and tribofilm effects.

Fig. 14a, corresponding to the nanolubricant TTM/IL/h-BN, shows the presence of the IL (blue) and h-BN (green) on the worn surface. The three spectra in Fig. 14a agree with the Raman spectrum of the neat IL (Fig. S2), with those of the worn surface lubricated with TTM (Fig. S5) and of h-BN [41] nanopowders. The Raman analyses of TTM/IL/GnP on the scar surface are shown in Fig. 14b where red and blue show the presence of GnP or TTM and IL, respectively. In this figure, the carbon spectrum agrees with the spectrum of the worn surface lubricated with TTM (Fig. S5) and that of the GnP nanopowders (Fig S3), presenting the peaks

corresponding to the D and G-bands, as well as an additional band (2D band) which indicates the presence of GnP. Moreover, the IL spectrum of Fig. 14b coincides with that of the pure IL (Fig. S2). Furthermore, it has been found that the GnP nanoadditives are placed along several furrows on the worn surface. Therefore, mending effect takes place also resulting in a smoother surface. From the mappings in Fig. 14, it can be concluded that the IL plays a more important role for TTM/IL/h-BN than for TTM/IL/GnP, due to its stronger concentration in the tribofilm of the worn surface. Taking into account Raman, SEM and roughness results it can be concluded that for both nanodispersions the main tribological mechanisms are the formation of the IL and nanoparticle tribofilms, as well as the mending effect due to nanoparticles. Thus, positive synergies between the nanoadditives and the IL were found.

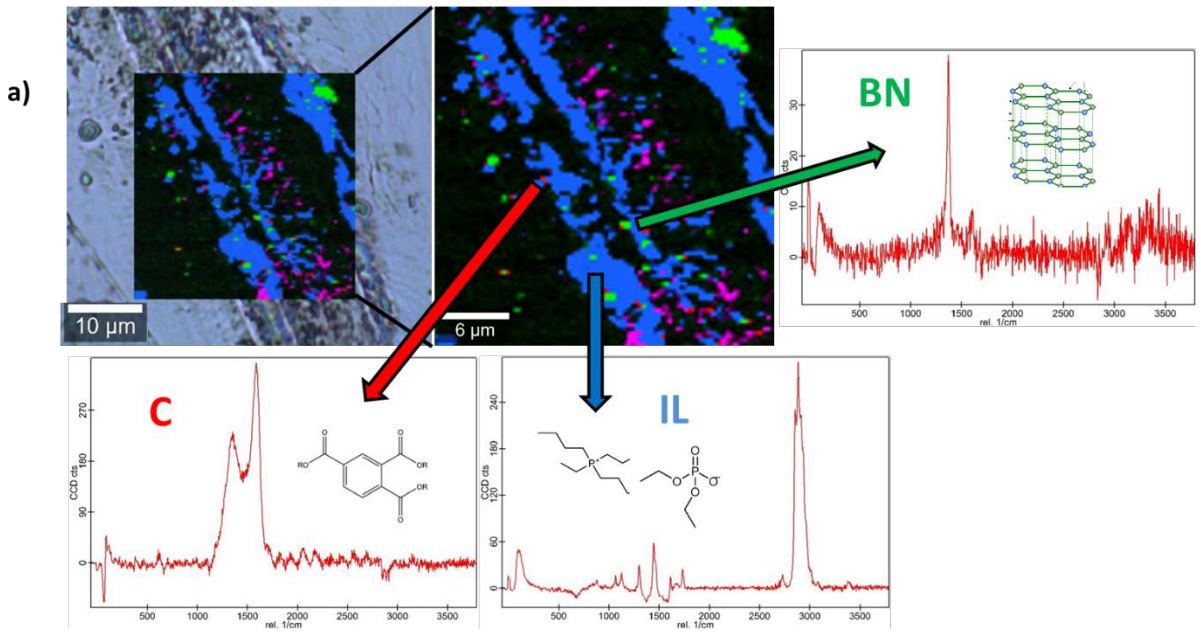

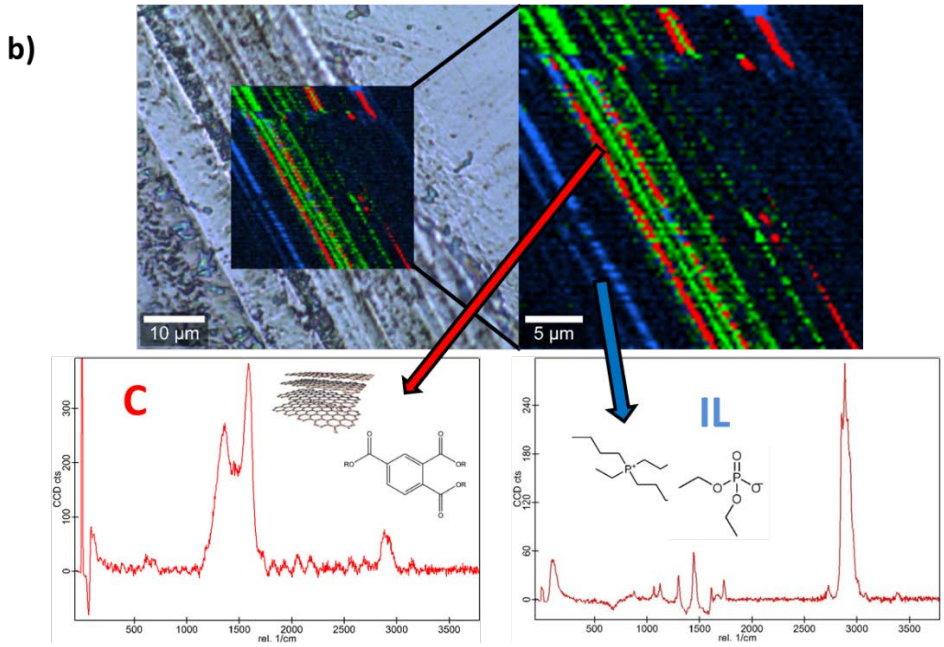

Fig. 14. Raman spectra and elemental map of the worn surface obtained with the nanolubricant a) TTM + 2 wt% IL + 0.1 wt% h-BN and b) TTM + 2 wt% IL + 0.1 wt% GnP

4. Conclusions

In this work the following features were achieved:

1. Dispersions based on graphene nanoplatelets, GnPs, or nanoparticles of hexagonal boron nitride, h-BN, with or without the IL tri(butyl) ethylphosphonium diethylphosphate in an ester type base oil, triisotridecyltrimellitate (TTM), were prepared. Three weeks after their preparation, none of the dispersions showed signs of instability.
2. Rotational tribological tests were performed with a CSM standard tribometer under a normal load of 20 N, the contact pair being AISI52100/AISI52100. The mean friction coefficients obtained lubricating the contact with each one of the dispersions are lower than the corresponding ones using TTM without additives. With respect to that obtained with the neat oil, the maximum reduction of the friction coefficient is 33%, reached with the TTM/IL/GnP nanodispersion. We should point out that there is no previous study of GnP dispersions combined with both IL and base oil.

3. Wear was evaluated in terms of the width (WTW), the depth (WTD) and cross-section area of the wear track, as well as the roughness of the worn surface. In comparison to those obtained with the neat oil, the maximum reductions of mean WTW (44%), the mean transversal area (66%) and the mean roughness (65%) correspond to the TTM/IL/GnP nanodispersion whereas that of the mean WTD (32%) is obtained with TTM/IL/h-BN. Tribofilm formation was confirmed by confocal Raman microscopy on the worn surfaces. The results obtained for TTM/IL/h-BN are better than the only previous study with dispersions Palm Olein TMP Ester/IL/h-BN at room temperature [32].
4. From the above results, it can be concluded that positive synergies between the IL and h-BN or GnP as additives of TTM are found.

Declaration of competing interest

None.

Acknowledgments

It is a pleasure to thank Dr. Alfredo Amigo and Dr. María J. G. Guimarey (both from Applied Physics Department, University of Santiago de Compostela) for kindly allowing to use a refractometer and provide us unpublished data, respectively. Authors acknowledge Verkol and Cytec Solvay Group for providing us the TTM and IL samples respectively. Authors would like to thank the use of RIAIDT-USC analytical facilities, especially to Mr. Ezequiel Vázquez for his useful advice. This work was supported by MINECO and the ERDF programme through ENE2014-55489-C2-1-R and ENE2017-86425-C2-2-R projects, and by the Xunta de Galicia (ED431E 2018/08, ED431D 2017/06 and GRC ED431C 2016/001). These funders also financed the acquisition of the 3D Optical Profile (UNST15-DE-3156).

References

[1] K. Holmberg, A. Erdemir, Influence of tribology on global energy consumption, costs and emissions, Friction 5 (2017) 263-284.

[2] S. Shahnazar, S. Bagheri, S.B.A. Hamid, Enhancing lubricant properties by nanoparticle additives, Int. J. Hydrogen Energy 41 (2016) 3153-3170.

[3] M.I.H.C. Abdullah, M.F.B. Abdollah, N. Tamaldin, H. Amiruddin, N.R.M. Nuri, Effect of hexagonal boron nitride nanoparticles as an additive on the extreme pressure properties of engine oil, Ind. Lubr. Tribol. 68 (2016) 441-445.

[4] O.N. Çelik, N. Ay, Y. Göncü, Effect of nano hexagonal boron nitride lubricant additives on the friction and wear properties of AISI 4140 steel, Particul. Sci. Technol. 31 (2013) 501-506.

[5] M.S. Charoo, M.F. Wani, Tribological properties of h-BN nanoparticles as lubricant additive on cylinder liner and piston ring, Lubr. Sci. 29 (2017) 241-254.

[6] C.J. Reeves, P.L. Menezes, Evaluation of boron nitride particles on the tribological performance of avocado and canola oil for energy conservation and sustainability, Int. J. Adv. Manuf. Technol. 89 (2017) 3475-3486.

[7] Q. Wan, Y. Jin, P. Sun, Y. Ding, Tribological behaviour of a lubricant oil containing boron nitride nanoparticles, Procedia Eng. 102 (2015) 1038-1045

[8] G.M. Ay, Y. Göncü, N. Ay, Environmentally friendly material: Hexagonal boron nitride, Journal of Boron 1 (2016) 66-73.

[9] F.U. Shah, S. Glavatskih, O.N. Antzutkin, Boron in Tribology: From Borates to Ionic Liquids, Tribol. Lett. 51 (2013) 281-301.

[10] T.Q.P. Vuong, S. Liu, A. Van der Lee, R. Cuscó, L. Artús, T. Michel, P. Valvin, J.H. Edgar, G. Cassabois, B. Gil, Isotope engineering of van der Waals interactions in hexagonal boron nitride, Nature Materials 17 (2017) 152.

[11] J.M. Liñeira del Río, M.J.G. Guimarey, M.J.P. Comuñas, E.R. López, A. Amigo, J. Fernández, Thermophysical and tribological properties of dispersions based on graphene and a trimethylolpropane trioleate oil, J. Mol. Liquids 268 (2018) 854-866.

[12] S.S.N. Azman, N.W.M. Zulkifli, H. Masjuki, M. Gulzar, R. Zahid, Study of tribological properties of lubricating oil blend added with graphene nanoplatelets, J. Mater. Res. 31 (2016) 1932-1938.

[13] W. Rashmi, M. Khalid, Y.L. Xiao, T.C.S.M. Gupta, G.Z. Arwin, Tribological studies on graphene/tmp based nanolubricant, JESTEC 12 (2017) 365-373.

[14] D.W. Chang, J.-B. Baek, Eco-friendly synthesis of graphene nanoplatelets, J. Mater. Chem. A 4 (2016) 15281-15293.

[15] M. Zonggang, L. Weimin, Z. Shuxiang, Z. Feng, Functional Room-temperature Ionic Liquids as Lubricants for an Aluminum-on-Steel System, Chemistry Letters 33 (2004) 524-525.

[16] Z. Mu, F. Zhou, S. Zhang, Y. Liang, W. Liu, Effect of the functional groups in ionic liquid molecules on the friction and wear behavior of aluminum alloy in lubricated aluminum-on-steel contact, Tribology International 38 (2005) 725-731.

[17] A.E. Jiménez, M.D. Bermúdez, P. Iglesias, F.J. Carrión, G. Martínez-Nicolás, 1-N-alkyl -3-methylimidazolium ionic liquids as neat lubricants and lubricant additives in steel–aluminium contacts, Wear 260 (2006) 766-782.

[18] A.E. Jiménez, M.D. Bermúdez, F.J. Carrión, G. Martínez-Nicolás, Room temperature ionic liquids as lubricant additives in steel–aluminium contacts: Influence of sliding velocity, normal load and temperature, Wear 261 (2006) 347-359.

[19] J. Qu, J.J. Truhan, S. Dai, H. Luo, P.J. Blau, Ionic liquids with ammonium cations as lubricants or additives, Tribology Letters 22 (2006) 207-214.

[20] A.-E. Jiménez, M.-D. Bermúdez, Ionic liquids as lubricants for steel–aluminum contacts at low and elevated temperatures, Tribology Letters 26 (2007) 53-60.

[21] B.A. Kheireddin, W. Lu, I.C. Chen, M. Akbulut, Inorganic nanoparticle-based ionic liquid lubricants, Wear 303 (2013) 185-190.

[22] M.-D. Avilés, N. Saurín, J. Sanes, F.-J. Carrión, M.-D. Bermúdez, Ionanocarbon Lubricants. The Combination of Ionic Liquids and Carbon Nanophases in Tribology, Lubricants 5 (2017) 14.
[23] Y. Zhou, J. Qu, Ionic liquids as lubricant additives: a review, ACS Appl. Mater. Interfaces 9 (2017) 3209-3222.
[24] I. Otero, E.R. López, M. Reichelt, M. Villanueva, J. Salgado, J. Fernández, Ionic Liquids Based on Phosphonium Cations As Neat Lubricants or Lubricant Additives for a Steel/Steel Contact, ACS Appl. Mater. Interfaces 6 (2014) 13115-13128.
[25] Y. Zhou, J. Dyck, T.W. Graham, H. Luo, D.N. Leonard, J. Qu, Ionic Liquids Composed of Phosphonium Cations and Organophosphate, Carboxylate, and Sulfonate Anions as Lubricant Antiwear Additives, Langmuir 30 (2014) 13301-13311.
[26] W.C. Barnhill, J. Qu, H. Luo, H.M. Meyer, C. Ma, M. Chi, B.L. Papke, Phosphonium-Organophosphate Ionic Liquids as Lubricant Additives: Effects of Cation Structure on Physicochemical and Tribological Characteristics, ACS Appl. Mater. Interfaces 6 (2014) 22585-22593.
[27] V. Khare, M.-Q. Pham, N. Kumari, H.-S. Yoon, C.-S. Kim, J.-I.L. Park, S.-H. Ahn, Graphene–Ionic Liquid Based Hybrid Nanomaterials as Novel Lubricant for Low Friction and Wear, ACS Applied Materials & Interfaces 5 (2013) 4063-4075.
[28] L. Zhang, J. Pu, L. Wang, Q. Xue, Synergistic Effect of Hybrid Carbon Nanotube–Graphene Oxide as Nanoadditive Enhancing the Frictional Properties of Ionic Liquids in High Vacuum, ACS Applied Materials & Interfaces 7 (2015) 8592-8600.
[29] Z. He, P. Alexandridis, Ionic liquid and nanoparticle hybrid systems: emerging applications, Adv. Colloid Interface Sci. 244 (2017) 54-70.
[30] A. Senatore, M. Pisaturo, D. Guida, Polyalkylene glycol based lubricants and tribological behaviour: role of ionic liquids and graphene oxide as additives, J. Nanosci. Nanotechnol. 18 (2018) 913-924.
[31] J. Sanes, M.-D. Avilés, N. Saurín, T. Espinosa, F.-J. Carrión, M.-D. Bermúdez, Synergy between graphene and ionic liquid lubricant additives, Tribol. Int. 116 (2017) 371-382.
[32] S.A.S. Amiril, E.A. Rahim, N. Talib, K. Kamdani, M.Z. Rahim, S. Syahrullail, Performance evaluation of palm-olein TMP ester containing hexagonal boron nitride and an oil miscible ionic liquid as bio-based metalworking fluids, J. Mech. Eng. SI 4 (2017) 223-234.
[33] Y. Li, S. Zhang, Q. Ding, H. Li, B. Qin, L. Hu, Understanding the synergistic lubrication effect of 2-mercaptobenzothiazolate based ionic liquids and Mo nanoparticles as hybrid additives, Tribol. Int. 125 (2018) 39-45.
[34] R.P. Swatloski, J.D. Holbrey, R.D. Rogers, Ionic liquids are not always green: hydrolysis of 1-butyl-3-methylimidazolium hexafluorophosphate, Green Chem. 5 (2003) 361-363.
[35] I. Minami, M. Kita, T. Kubo, H. Nanao, S. Mori, The Tribological Properties of Ionic Liquids Composed of Trifluorotris(pentafluoroethyl) Phosphate as a Hydrophobic Anion, Tribol. Lett. 30 (2008) 215-223.
[36] I. Otero, E.R. López, M. Reichelt, J. Fernández, Friction and anti-wear properties of two tris(pentafluoroethyl)trifluorophosphate ionic liquids as neat lubricants, Tribol. Int. 70 (2014) 104-111.
[37] P. Oulego, D. Blanco, D. Ramos, J.L. Viesca, M. Díaz, A. Hernández Battez, Environmental properties of phosphonium, imidazolium and ammonium cation-based ionic liquids as potential lubricant additives, J. Mol. Liquids 272 (2018) 937-947.
[38] L.R. Rudnick, Synthetics, Mineral Oils, and Bio-Based Lubricants: Chemistry and Technology (2013).
[39] H. Lai, Z. Wang, P. Wu, B.I. Chaudhary, S.S. Sengupta, J.M. Cogen, B. Li, Structure and Diffusion Behavior of Trioctyl Trimellitate (TOTM) in PVC Film Studied by ATR-IR Spectroscopy, Ind. Eng. Chem. Res. 51 (2012) 9365-9375.
[40] X.-H. Guan, G.-H. Chen, C. Shang, Combining kinetic investigation with surface spectroscopic examination to study the role of aromatic carboxyl groups in NOM adsorption by aluminum hydroxide, J. Colloid Interf. Sci. 301 (2006) 419-427.

[41] J.M. Liñeira del Río, M.J.G. Guimarey, M.J.P. Comuñas, E.R. López, J.I. Prado, L. Lugo, J. Fernández, Thermophysical and tribological properties of environmentally-friendly lubricants based on trimethylolpropane trioleate with hexagonal boron nitride nanoparticles as additive, Coatings 9 (2019) 509.
[42] A. Hernández Battez, M. Bartolomé, D. Blanco, J.L. Viesca, A. Fernández-González, R. González, Phosphonium cation-based ionic liquids as neat lubricants: Physicochemical and tribological performance, Tribol. Int. 95 (2016).
[43] J.M. Liñeira del Río, E.R. López, J. Fernández, F. García, Tribological properties of dispersions based on reduced graphene oxide sheets and trimethylolpropane trioleate or PAO 40 oils, J. Mol. Liquids 274 (2019) 568-576.
[44] F. Novotny-Farkas, W. Böhme, H. Stabinger, W. Belitsch, The Stabinger Viscometer a new and unique instrument for oil service laboratories, Anton Paar, World Tribology Congress II, Vienna, Austria, 2001.
[45] X. Paredes, O. Fandiño, M.J.P. Comuñas, A.S. Pensado, J. Fernández, Study of the effects of pressure on the viscosity and density of diisodecyl phthalate, J. Chem. Thermodyn. 41 (2009) 1007-1015.
[46] F.M. Gaciño, T. Regueira, L. Lugo, M.J.P. Comuñas, J. Fernández, Influence of Molecular Structure on Densities and Viscosities of Several Ionic Liquids, J. Chem. Eng. Data 56 (2011) 4984-4999.
[47] M.J.G. Guimarey, M.J.P. Comuñas, E.R. López, A. Amigo, J. Fernández, Thermophysical properties of polyalphaolefin oil modified with nanoadditives, J. Chem. Thermodyn. 131 (2019) 192-205.
[48] M.J.G. Guimarey, M.R. Salgado, M.J.P. Comuñas, E.R. López, A. Amigo, D. Cabaleiro, L. Lugo, J. Fernández, Effect of ZrO2 nanoparticles on thermophysical and rheological properties of three synthetic oils, J. Mol. Liquids 262 (2018) 126-138.
[49] K. Lee, Y. Hwang, S. Cheong, Y. Choi, L. Kwon, J. Lee, S.H. Kim, Understanding the Role of Nanoparticles in Nano-oil Lubrication, Tribol. Lett. 35 (2009) 127-131.
[50] M. Gulzar, H.H. Masjuki, M.A. Kalam, M. Varman, N.W.M. Zulkifli, R.A. Mufti, R. Zahid, Tribological performance of nanoparticles as lubricating oil additives, J. Nanopart. Res. 18 (2016) 223.
[51] R.V. Gorbachev, I. Riaz, R.R. Nair, R. Jalil, L. Britnell, B.D. Belle, E.W. Hill, K.S. Novoselov, K. Watanabe, T. Taniguchi, A.K. Geim, P. Blake, Hunting for Monolayer Boron Nitride: Optical and Raman Signatures, Small 7 (2011) 465-468.
[52] A.C. Ferrari, J.C. Meyer, V. Scardaci, C. Casiraghi, M. Lazzeri, F. Mauri, S. Piscanec, D. Jiang, K.S. Novoselov, S. Roth, A.K. Geim, Raman Spectrum of Graphene and Graphene Layers, Phys. Rev. Lett. 97 (2006) 187401.